Self-Assembly on Surfaces

Supramolecular Patterned Surfaces Driven by Cooperative Assembly of C_{60} and Porphyrins on Metal Substrates**

Davide Bonifazi, Hannes Spillmann, Andreas Kiebele, Michael de Wild, Paul Seiler, Fuyong Cheng, Hans-Joachim Güntherodt, Thomas Jung,* and François Diederich**

Systems that spontaneously self-organize through selective interactions into extended supramolecular entities offer a number of powerful approaches for the development of functional-molecule-based devices.[1] Selective noncovalent interactions have been widely exploited both in solution and in the solid state to prepare extended assemblies in one (polymolecular chains and fibers),[2,3] two (arrays, layers, and membranes),[3,4] and three dimensions.[5] Recently this concept has been extended to the surface engineering of multidimensional assemblies[6] stabilized by hydrogen-bonding,[7] dipole–dipole,[8] donor–acceptor,[9] and van der Waals[10] interactions.

π-Conjugated molecules such as fullerenes and porphyrins with tunable electronic properties are appealing building blocks for the construction of functional materials with exceptional electrochemical and photophysical properties.[11] One of the most interesting aspects of C_{60} and porphyrins is that they spontaneously attract each other mainly through orbital interactions, as experimentally determined in so-

[*] Dr. H. Spillmann, A. Kiebele, Dr. M. de Wild, Prof. Dr. H.-J. Güntherodt
NCCR Nanoscale Science
Department of Physics, University of Basel
Klingelbergstrasse 82, 4056 Basel (Switzerland)
Fax: (+41) 61-267-3784
E-mail: h.spillmann@unibas.ch

Dr. T. Jung
Laboratory for Micro- and Nanotechnology
Paul Scherrer Institute
5232 Villigen PSI (Switzerland)
Fax: (+41) 56-310-2646
E-mail: thomas.jung@psi.ch

D. Bonifazi, Dr. P. Seiler, Dr. F. Cheng, Prof. Dr. F. Diederich
Laboratorium für Organische Chemie
ETH-Hönggerberg, HCI
8093 Zürich (Switzerland)
Fax: (+41) 1-632-1109
E-mail: diederich@org.chem.ethz.ch

[**] We gratefully acknowledge the financial support from the Swiss National Science Foundation, the NCCR "Nanoscience", and the Swiss Federal Commission for Technology and Innovation (KTI). We also thank Nanonis Inc. for their fruitful collaboration on the data acquisition and molecular positioning system.

Supporting information (X-ray crystal structure of **2**, STM studies on monolayers of a triply fused diporphyrin with two 4-cyanophenyl residues, and movies illustrating dynamic processes) for this article is available on the WWW under http://www.angewandte.org or from the author.

 DOI: 10.1002/ange.200460562

lution[12] and in the solid state,[13] and confirmed by high-level calculations.[14] In earlier reports we evidenced that the attractive C_{60}–porphyrin interaction substantially affects the conformational, electrochemical, and photophysical properties of covalent conjugates.[15–17] However, the study of the C_{60}–porphyrin interaction on solid surfaces is largely unexplored.[18] The formation of self-assembled molecular layers that are weakly physisorbed on surfaces provides the conceptional basis to engineer addressable fullerene–porphyrin architectures in which both chromophores are proximally assembled by noncovalent interactions. Herein we report on the bottom-up fabrication of patterned surfaces based on unprecedented two-dimensional (2D) supramolecular assemblies composed of porphyrins and C_{60}. The first scanning tunneling microscopy (STM) studies on monolayers of triply fused and monomeric porphyrins show that **1**[17,19] and **2** (Scheme 1) self-organize into ordered molecular bilayers upon co-deposition with C_{60}. Repositioning experiments[20] conducted with the STM tip demonstrate that the C_{60} molecules are weakly adsorbed onto the porphyrin monolayers and they can be easily relocated without disrupting the underlying layer.

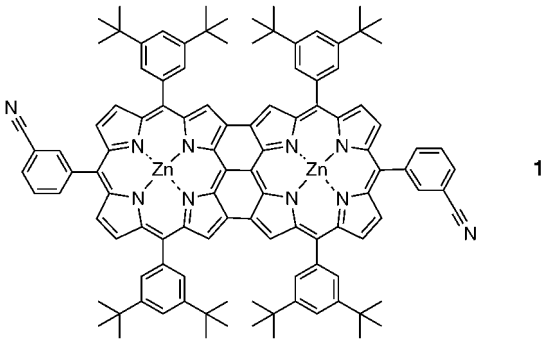

Scheme 1. Chemical structure of the porphyrin derivatives prepared according to the synthetic protocols recently reported.[17]

The first step in the formation of the self-assembled patterned surfaces is the deposition of the porphyrin macrocycles onto an Ag(100) surface under ultrahigh vacuum (UHV).[21] High-resolution STM images taken on an Ag(100) substrate covered with a 0.2–0.5 monolayer of diporphyrin **1** showed the coexistence of two phases: 2D ordered islands in dynamic equilibrium with a 2D gas phase. Evidence for this 2D molecular gas phase was obtained from the fluctuation of the borders of the condensed islands in time-lapse imaging sequences (see the Supporting Information).[22] The individual molecules in the STM images are represented as groups of four lobes arranged in a slightly distorted square shape (Figure 1 a, left). According to earlier experiments conducted on tetra-arylated porphyrins,[18] each lobe in the STM image results from preferential tunneling transport through the 3,5-di(*tert*-butyl)phenyl substituents.[23] The observed size of the four-lobed shape is about $1.1 \times 0.8\ nm^2$, which is consistent with the molecular dimensions of **1**, as estimated by PM3-

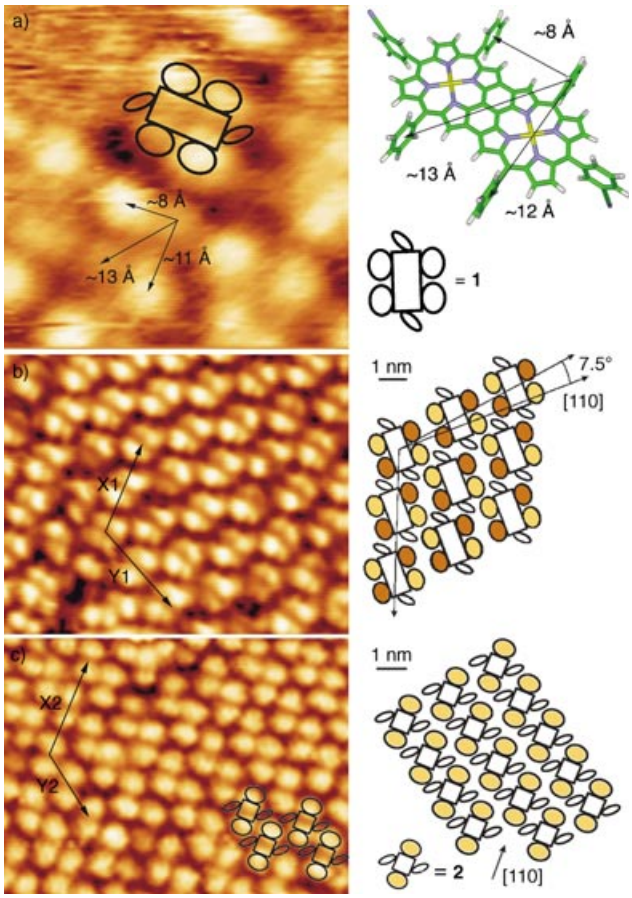

Figure 1. a) Left: STM image (scan range: $5.0 \times 5.0\ nm^2$, $V_{bias} = 2.57$ V, $I_t = 21$ pA, $T = 298$ K) of a single molecule of diporphyrin **1** sublimed on Ag(100) in proximity to a 2D mobile molecular phase.[22] Right: optimized molecular structure of porphyrin **1** generated by PM3 calculations implemented within Spartan (the *tert*-butyl functionalities have been omitted for clarity). b) Left: STM image (scan range: $15.8 \times 11.9\ nm^2$, $V_{bias} = 2.5$ V, $I_t = 72$ pA, $T = 298$ K) of a full-coverage monolayer of **1** sublimed on Ag(100); the distance between the centers of two neighboring molecules is 2.2 ± 0.1 nm along the X1 direction and 2.3 ± 0.1 nm along the Y1 direction; the molecular rows cross each other at an angle of $120 \pm 5°$ along the direction X1 and Y1. Right: proposed surface pattern of the self-assembled monolayer on Ag(100) (the yellow and brown lobes reflect the heights attributed to the different conformation adopted by the 3,5-di(*tert*-butyl)phenyl legs as displayed by the dissimilar intensity tunneling current). c) Left: STM image (scan range: $12.2 \times 9.1\ nm^2$, $V_{bias} = 2.80$ V, $I_t = 72$ pA, $T = 298$ K) of a full-coverage monolayer of porphyrin **2** sublimed on Ag(100); the distance between the centers of two neighboring molecular subunits is 2.4 ± 0.1 nm along the X2 direction and 1.5 ± 0.1 nm along the Y2 direction; the molecular rows along the direction X2 and Y2 cross each other at an angle of $126 \pm 5°$. Right: proposed surface pattern of the self-assembled molecular layer on Ag(100).

based geometry optimization (Figure 1a, right). Although the rotation of the 3,5-di(*tert*-butyl)phenyl substituents about the phenyl–porphyrin σ bond is sterically hindered at small interplanar angles, they still have a certain degree of freedom to partially rotate without affecting each other. Therefore, the reason why the four protrusions appear with distinct heights is attributable to a different conformation being adopted by the four 3,5-di(*tert*-butyl)phenyl moieties.[23] To confirm such conformational arguments a triply linked diporphyrin bearing two 4-cyanophenyl substituents was also synthesized as a reference compound, and the results are consistent with our interpretations (see the Supporting Information). At higher coverage (ca. 1.0 monolayer), diporphyrin **1** self-organizes in regular molecular rows that are clearly distinguishable in the STM images (Figure 1b, left), which are characterized by a high packing density.

Compound **2** was also sublimed on Ag(100) under the same conditions. Each molecule is represented as two aligned lobes which correspond to the 3,5-di(*tert*-butyl)phenyl substituents (Figure 1c, left). The distance between two bright lobes is about 1.1 nm, which is in agreement with the intramolecular distance between the 3,5-di(*tert*-butyl)phenyl moieties as measured in the crystal structure of **2** (see the Supporting Information). In analogy to **1**, the porphyrin central core and the 3-cyanophenyl residues are not visible on a single-molecule image. Again a 2D gas phase was observed in equilibrium with the ordered islands, thus showing that the porphyrin–substrate and porphyrin–porphyrin interactions at 298 K are similar for both compounds **1** and **2**. At complete surface coverage (ca. 1.0 monolayer) the molecules arrange themselves into rows along the ⟨110⟩ direction of the underlying Ag(100) substrate (Figure 1c, right). In contrast to **1**, all the lobes appear with the same height, which suggests that the interplanar angle between the 3,5-di(*tert*-butyl)phenyl moiety and the porphyrin plane is equal for all molecules within the monolayer.

Sublimation of an approximately 0.02 monolayer of C_{60} on top of a full monolayer of **1** on Ag(100) resulted in the predominant formation of unidirectional chains of various lengths composed of several bright protrusions (Figure 2a, left).[24] Each protrusion has a height of 4.4 ± 0.2 Å (measured with respect to the porphyrin layer). These protrusions can clearly be identified from their spherical appearance in the STM data as single C_{60} molecules.[25] The longest chains (ca. 15.5 nm) are composed of eight C_{60} molecules with an intermolecular $C_{60}\cdots C_{60}$ distance of about 2.2 nm. Surprisingly, no 2D islands composed of C_{60} have been detected. The superstructure of the bimolecular C_{60}–diporphyrin assembly (Figure 2a, left) which best fits the experimental data is also depicted (Figure 2a, right). Despite the large surface area of the fused macrocyclic core (ca. 1 nm^2), the fullerene-based chains are formed by molecules which are located outside of the porphyrin macrocycles, precisely on top of the 3-cyanophenyl substituents.

To exclude the possibility that the C_{60} molecules are embedded in the porphyrin domains as self-intermixed phase, for example, such as in subphthalocyanine and C_{60} assemblies,[26] single-molecule repositioning experiments of the carbon spheres were performed. Figure 2b shows the STM

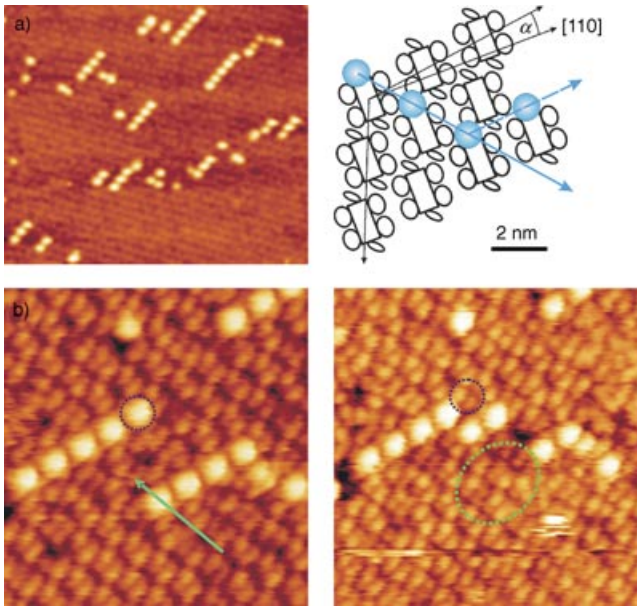

Figure 2. STM images of **1**–C_{60} assembly. a) Left: STM images showing the preferential direction of the chainlike assembly of C_{60} on a previously deposited monolayer of **1** (scan range: 77×65 nm^2, $I_t = 22$ pA, $V_{bias} = 2.59$ V). Right: proposed model for the chainlike assembly (α = ca. 7.5°); the C_{60} molecules (blue spheres) are located between the diporphyrin molecules approximately on top of the 3-cyanophenyl residues; the solid blue and dashed blue arrow indicates the major and minor growth direction, respectively. b) Detailed view before (left) and after (right) manipulation sequence of the C_{60} molecule on a layer of **1** (scan range: 21×21 nm^2, $I_t = 11$ pA, $V_{bias} = 3.01$ V). The green arrow traces the lateral displacements of the STM tip during the manipulation (tunneling parameters: $I_t = 214$ pA, $V_{bias} = 1.43$ V, $V_{tip} = 5$ $nm\,s^{-1}$) and the green ellipse indicates the intact layer of **1** after repositioning of the C_{60} molecule; the blue circle denotes a C_{60} molecule that vanished during the repositioning experiment.

images recorded before (left) and after (right) C_{60} repositioning on a full monolayer of **1**. After the relocation sequence, the former fullerene site (green ellipse in Figure 2b, right) is clearly occupied only by **1**, thus proving that the C_{60} molecules sit on top of the monolayer. Interestingly all attempts toward the formation of square islands composed of four carbon spheres failed, but led to the abstraction of a C_{60} molecule, as evident with the fullerene molecule positioned at the end of the left chain (blue circle in Figure 2b). The latter observation hints at an intrinsic property of such layers of **1**: condensed 2D phases composed of C_{60} molecules are energetically unfavored and only chainlike phases are preferred.

Deposition of an approximately 0.14 monolayer of C_{60} onto a preadsorbed approximately 0.85 monolayer of **2** on an Ag(111) substrate resulted in the formation of two segregate molecular domains: 1) $2\sqrt{3} \times 2\sqrt{3}$ R30° islands[27,28] of C_{60} and 2) a condensed phase composed of **2**. Thermal annealing (453 K) of samples containing such segregate domains afforded the unprecedented porphyrin–C_{60} assembly shown in Figure 3 as the main phase. The carbon spheres are arranged in vertically aligned pairs (intrapair $C_{60}\cdots C_{60}$ distance of 2.3 nm) which are separated by about 6.0 nm. This paired line pattern is repeated every 7.3 nm in the horizontal direction and results in exceptionally large domains (up to

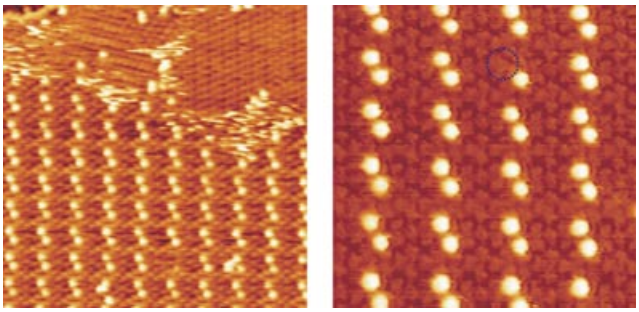

Figure 3. STM image of **1**–C_{60} assembly. Left: STM image of the 2D arrangement of C_{60} on a monolayer of **2** (scan range: 68×68 nm^2, $I_t = 64$ pA, $V_{bias} = 1.97$ V). Right: detailed view (scan range: 30×30 nm^2, $I_t = 16$ pA, $V_{bias} = 2.67$ V); the blue circle indicates a C_{60} vacancy.

50×100 nm^2). Notably the presence of an undistorted monolayer of **2** in the proximity of the fullerene vacancy (blue circle in Figure 3, right), supports the assumption that the C_{60} molecules are accommodated on top of the porphyrin layer. In the upper part of Figure 3 (left), isolated domains of **2** on Ag(111) with some loose C_{60} molecules are visible (see also the Supporting Information). Noisy areas consisting of spikes with an apparent height similar to that of C_{60} molecules at the boundary of the porphyrin domains are indicative of loosely bound C_{60} molecules which are moving on the porphyrin layer at a frequency similar to the one of the STM tip.[22] The shape and apparent height of such bright protrusions (4.8 ± 0.3 Å) are very similar to those found for the C_{60} spheres on top of the layer of **1**. While the monolayer of **1** does not reorder upon deposition of C_{60}, the monolayer of **2** reorganizes upon formation of the hybrid **2**–C_{60} assembly (see top part on Figure 3 (left) and Supporting Information).

Notably while the assembly of C_{60} and **1** is disrupted at 423 K, the assembly of C_{60} and **2** is formed at 453 K. The C_{60} molecules do not diffuse within both assemblies at 298 K. This observation indicates that the energy barrier for diffusion of the C_{60} molecules is larger than the thermal energy at 298 K. The large $C_{60}\cdots C_{60}$ distance in both superstructures excludes the presence of any significant contribution from the cohesive $C_{60}\cdots C_{60}$ energy, which is of the order of 31 kcal mol^{-1} at a separation of about 1 nm.[29] Moreover, in agreement with previous studies in solution,[17] any strong fullerene–porphyrin interactions are absent in the assembly of diporphyrin **1**, since the C_{60} molecules are not located directly above the macrocyclic cores and can be repositioned without altering the underlying porphyrin layer (see Figure 2 b).

Evidence for a unique type of interplay can be deduced by time-lapsed series of STM images of a full-coverage monolayer of a tetra-arylated porphyrin (see the Supporting Information). Fluctuating bright/dim patterns which are attributed to rotations of the 3,5-di(*tert*-butyl)phenyl substituents of neighboring molecules were observed. These conformational changes are most likely based on van der Waals interactions and propagate within the monolayer from one molecule to its neighbors. The same interpretation can be assigned to the formation of chains of C_{60} molecules on a monolayer of **1**. In this assembly, C_{60}-induced conformational changes of the 3,5-di(*tert*-butyl)phenyl substituents propagate in the underlying porphyrin layer, thus directing the formation of fullerene chains on top of it.

In contrast to the chainlike assembly, we could not precisely estimate the location of the C_{60} molecules with respect to the underlying monolayer of **2** within the **2**–C_{60} assembly. Nevertheless, the high thermal stability and the long-range order accounts for a strong interaction within the assembly that we tentatively ascribe to the rather high porphyrin–fullerene interaction energy (of the order of 16–18 kcal mol^{-1} for monomeric porphyrin).[14] These conclusions are in agreement with our recent results obtained in solution, which show that monomeric porphyrins such as **2** undergo much stronger interchromophoric interactions with C_{60} than triply fused diporphyrins such as **1**.[15,17]

In summary, the first example of addressable supramolecular architectures was obtained by self-assembly of fullerenes and porphyrins on surfaces. The arrangement of the fullerene molecules on the patterned layer can be controlled by the porphyrin structure. The observed mode of self-assembly results from a delicate balance between the fullerene–porphyrin interaction and the conformational motion within the underlaying porphyrin layer. In addition to the exceptional molecular properties that can be embedded on the surface, such systems offer a valid alternative toward the construction of identical addressable molecular architectures. This is hardly imaginable by using established miniaturizing methods, such as the "lithographic" techniques, and provides an exceptional example of the potential of the supramolecular approach for the fabrication of laterally addressable molecular devices.

Received: May 5, 2004

Keywords: fullerenes · porphyrinoids · scanning probe microscopy · self-assembly · surface chemistry

[1] J.-M. Lehn, *Science* **2002**, *295*, 2400–2403.
[2] O. Ikkala, G. ten Brinke, *Science* **2002**, *295*, 2407–2409.
[3] D. N. Reinhoudt, M. Crego-Calama, *Science* **2002**, *295*, 2403–2407.
[4] G. M. Whitesides, B. Grzybowski, *Science* **2002**, *295*, 2418–2421.
[5] a) M. D. Hollingsworth, *Science* **2002**, *295*, 2410–2413; b) T. Kato, *Science* **2002**, *295*, 2414–2418.
[6] F. C. De Schryver, S. De Feyeter, *Chem. Soc. Rev.* **2003**, *32*, 139–150.
[7] a) M. Furukawa, H. Tanaka, K. Sugiura, Y. Sakata, T. Kawai, *Surf. Sci.* **2000**, *445*, L58–L63; b) J. A. Theobald, N. S. Oxtoby, M. A. Phillips, N. R. Champness, P. H. Beton, *Nature* **2003**, *424*, 1029–1031; c) J. Weckesser, A. D. Vita, J. V. Barth, C. Cai, K. Kern, *Phys. Rev. Lett.* **2001**, *87*, 096101; d) M. Böhringer, W.-D. Schneider, R. Berndt, *Surf. Rev. Lett.* **2000**, *7*, 661–663; e) S. De Feyter, M. Larsson, N. Schuurmans, B. Verkuijl, G. Zoriniants, A. Gesquiere, M. M. Abdel-Mottaleb, J. van Esch, B. L. Feringa, J. van Stam, F. De Schryver, *Chem. Eur. J.* **2003**, *9*, 1198–1206.
[8] a) T. Yokoyama, S. Yokoyama, T. Kamikado, Y. Okuno, S. Mashiko, *Nature* **2001**, *413*, 619–621; b) K. Morgenstern, E. Laegsgaard, I. Stensgaard, F. Besenbacher, M. Böhringer, W.-D. Schneider, R. Berndt, F. Mauri, A. D. Vita, R. Car, *Appl. Phys. A* **1999**, *69*, 559–663.

[9] a) P. Samori, X. M. Yin, N. Tchebotareva, Z. H. Wang, T. Pakula, F. Jackel, M. D. Watson, A. Venturini, K. Mullen, J. P. Rabe, *J. Am. Chem. Soc.* **2004**, *126*, 3567 – 3575; b) M. Stöhr, T. Wagner, M. Gabriel, B. Weyers, R. Möller, *Adv. Funct. Mater.* **2001**, *11*, 175 – 178.
[10] a) M. Schunack, L. Petersen, A. Kühnle, E. Lægsgaard, I. Stensgaard, I. Johannsen, F. Besenbacher, *Phys. Rev. Lett.* **2001**, *86*, 456 – 459; b) M. Böhringer, K. Morgenstern, W.-D. Schneider, R. Berndt, F. Mauri, A. D. Vita, R. Car, *Phys. Rev. Lett.* **1999**, *83*, 324 – 327.
[11] R. E. Martin, F. Diederich, *Angew. Chem.* **1999**, *111*, 1440 – 1469; *Angew. Chem. Int. Ed.* **1999**, *38*, 1350 – 1377.
[12] a) J. Xiao, M. E. Meyerhoff, *J. Chromatogr. A* **1995**, *715*, 19 – 29; b) M. Ayabe, A. Ikeda, Y. Kubo, M. Takeuchi, S. Shinkai, *Angew. Chem.* **2002**, *114*, 2914 – 2916; *Angew. Chem. Int. Ed.* **2002**, *41*, 2790 – 2792.
[13] a) D. Sun, F. S. Tham, C. A. Reed, P. D. W. Boyd, *Proc. Natl. Acad. Sci. USA* **2002**, *99*, 5088 – 5092; b) D. Y. Sun, F. S. Tham, C. A. Reed, L. Chaker, P. D. W. Boyd, *J. Am. Chem. Soc.* **2002**, *124*, 6604 – 6612.
[14] Y.-B. Wang, Z. Lin, *J. Am. Chem. Soc.* **2003**, *125*, 6072 – 6073.
[15] N. Armaroli, G. Marconi, L. Echegoyen, J. P. Bourgeois, F. Diederich, *Chem. Eur. J.* **2000**, *6*, 1629 – 1645.
[16] D. Bonifazi, F. Diederich, *Chem. Commun.* **2002**, 2178 – 2179.
[17] D. Bonifazi, M. Scholl, F. Y. Song, L. Echegoyen, G. Accorsi, N. Armaroli, F. Diederich, *Angew. Chem.* **2003**, *115*, 5116 – 5120; *Angew. Chem. Int. Ed.* **2003**, *42*, 4966 – 4970.
[18] J. K. Gimzewski, T. A. Jung, M. T. Cuberes, R. R. Schlitter, *Surf. Sci.* **1997**, *386*, 101 – 114.
[19] A. Tsuda, H. Furuta, A. Osuka, *Angew. Chem.* **2000**, *112*, 2649 – 2652; *Angew. Chem. Int. Ed.* **2000**, *39*, 2549 – 2551.
[20] T. A. Jung, R. R. Schlitter, J. K. Gimzewski, H. Tang, C. Joachim, *Science* **1996**, *271*, 181 – 184.
[21] The porphyrins as well as C_{60} were deposited on the metal substrates in a standard UHV chamber ($P_{base} = 2 \times 10^{-10}$ mbar). Flat Ag(100) and Ag(111) terraces (up to 200 nm of width) separated by monoatomic steps were prepared by repeated cycles (ca. 15 min) of Ar^+ sputtering and thermal annealing (ca. 870 K). All molecules were transferred onto the silver surfaces (kept at 298 K) by organic molecular beam deposition from a Knudsen-cell-type evaporator with a deposition rate of about 0.3 monolayer min^{-1}. The rate was controlled by a quartz microbalance which was calibrated with STM images of ordered areas. Room-temperature STM experiments employing constant current mode were performed in situ after the deposition of the molecular layer with a chemically etched tungsten tip and with an in-house built microscope (comparable to the OMICRON design). Typical scan rates were in the range of 2–4 Hz per scanline. The chemical composition of the layers was confirmed by X-ray photoelectron spectroscopy.
[22] S. Berner, M. de Wild, L. Ramoino, S. Ivan, A. Baratoff, H.-J. Güntherodt, H. Suzuki, D. Schlettwein, T. A. Jung, *Phys. Rev. B* **2003**, *68*, 115410.
[23] a) T. A. Jung, R. R. Schlitter, J. K. Gimzewski, *Nature* **1997**, *386*, 696 – 698; b) J. Kuntze, X. Ge, R. Berndt, *Nanotechnology* **2002**, *15*, S337-S340.
[24] Chains consisting of a maximum of three C_{60} molecules tilted at an angle of $120 \pm 4°$ (dashed blue arrow in Figure 2a, right) with respect to the main direction of the fullerene chains (blue arrow in Figure 2a, right) have also been observed in the STM images.
[25] The C_{60} molecules appear with a diameter of approximately 1.5 nm (van der Waals diameter of C_{60} is ca. 1 nm) because of the tip–molecule convolution that broadens the lateral dimensions of single objects in STM.
[26] M. de Wild, S. Berner, H. Suzuki, H. Yanagi, D. Schlettwein, S. Ivan, A. Baratoff, H.-J. Güntherodt, T. A. Jung, *ChemPhysChem* **2002**, *3*, 881 – 885.
[27] E. I. Altman, R. J. Colton, *Phys. Rev. B* **1993**, *48*, 18244 – 18249.
[28] C. Ton-That, A. G. Shard, S. Egger, V. R. Dhanak, M. E. Welland, *Phys. Rev. B* **2003**, *67*, 155415.
[29] a) C. Pan, M. P. Sampson, Y. Chai, R. H. Hauge, J. L. Margrave, *J. Phys. Chem.* **1991**, *95*, 2944 – 2946; b) X. Shi, W. B. Caldwell, K. Chen, C. A. Mirkin, *J. Am. Chem. Soc.* **1994**, *116*, 11598 – 11599.

